A QUANTITATIVE SMALL-SCALE CHARACTERIZATION SUITE TO ASSESS HYBRID-MANUFACTURED TOOLING DURABILITY FOR COMPOSITE PROCESSES

Ilse, J.[1,2], Hubert, P.[1,2]*
[1] Department of Mechanical Engineering, McGill University, Montreal, Canada
[2] Research Centre for High Performance Polymer and Composite Systems CREPEC, Montreal, Canada
* Corresponding author (pascal.hubert@mcgill.ca)

Keywords*: additive manufacturing, tooling, durability*

ABSTRACT

In traditional tool manufacturing there exist inherent material or labour costs when using high performance metal or composite materials respectively. Hybridized large-scale additive and subtractive processing, in which a thermoplastic material extrusion system is combined with conventional CNC machine, allows for printing of near-net shapes and their subsequent machining to take place on the same machine. This allows for reduced lead time and labour enabling rapid tool development and production. To assess durability of tools produced through this process however, most research and development is performed through large-scale empirical testing which leads to superfluous time expenditure, material waste, and associated costs. There is a need for less time and material-intensive approach to characterize tool durability.

This work presents a small-scale suite of characterization methods to quantitatively assess hybrid-manufactured tool durability for composite part fabrication. Durability is evaluated in the context of vacuum infusion processing, where mechanical resistance, chemical resistance, and vacuum integrity are investigated. Corresponding characterization tools employed are hardness testing, tensiometry, and a custom vacuum test. Results can be used as an early-stage screening process in design and manufacturing of large-scale tooling produced through hybrid manufacturing before progressing onto more time, material, and cost-intensive large-scale testing methods.

1 INTRODUCTION

Tooling is an essential element in almost all composite processes in which tight control of the tool properties is required to ensure good quality composite parts. Traditionally these tools are manufactured using metal or composite materials, both of which offer advantages and disadvantages in properties and performance depending on the composite process employed [1, 2]. However, an underlying theme among both are high costs associated with fabrication, due to either inherent material or labour costs when using high performance metal alloys or composite materials respectively [1, 2].

Recent studies have looked at using hybridized large-scale additive and subtractive processing to address these shortcomings in tool manufacturing. Hybridized large-scale additive and subtractive processing, in which a thermoplastic material extrusion system is combined with conventional CNC machine, allows for printing of near-net shapes and their subsequent machining to take place on the same machine [3, 4, 5]. This hybridized process allows for reduced lead time and labour enabling rapid tool development and production. To assess the durability of tools produced through this process however, most research and development is typically performed through large-scale empirical testing which leads to superfluous time expenditure, material waste, and associated costs [3, 4, 5]. There is a need for less time and material-intensive approach to characterize tool durability.

The aim of this paper is to present a small-scale suite of characterization methods to quantitatively assess and predict the durability of hybrid-manufactured tools for composite part fabrication. Tool durability is evaluated with respect to three key aspects: mechanical resistance, chemical resistance, and vacuum integrity. The corresponding characterization tools employed are hardness/micro-indentation testing, advancing-receding contact angle (ARCA) tensiometry, and a custom vacuum test used to perform a 5-minute “drop test”. The results of these tests can be used as an early-stage screening process in the design and manufacturing of large-scale tooling produced through the hybrid manufacturing process before progressing onto more time, material, and cost-intensive large-scale testing methods.

2 Materials & Methodology

2.1 Tool Fabrication

For all tests, a single type of test specimen was fabricated, hereafter referred to as a “tool” or “specimen”. These tools consisted of a base material followed by the application of a coating or left uncoated (Figure 1). A total of 3 different tool materials and 5 coating combinations (including uncoated) were fabricated for a total of 6 unique tool-coating combinations (Table 1). The dimensions of the tool were 25.4 mm x 25.4 mm in terms of length and width with varying heights depending on the tool material and its associated manufacturing method. Tool thickness was not important as it did not influence any of the test results. Following the fabrication of the base tool substrates, one 25.4 mm x 25.4 mm surface on each was machined and polished to a surface finish of 500 grit prior to the application of any coating. This was done with the intent that the surface finish for all tools was equal and did not influence test results.

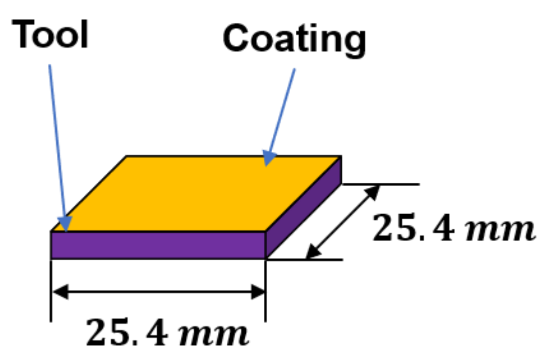

Figure 1. Tool geometry.

Table 1. Test matrix containing all possible tool-coating combinations and the associated tool material and coating. S1: Sealant 1, U: Uncoated, C-P: Ceramic-Polymer, S2: Sealant 2, E: Epoxy-Based.

Specimen ID	Tool Material	Tool Type	Coating
AL (S1)	Aluminum	Traditional (Metal)	Mould Sealant 1
GF-Epoxy (S1)	GF-Epoxy	Traditional (Composite)	Mould Sealant 1 Ceramic-Polymer
CF-ABS (U)	3D-CFABS	Hybrid	None
CF-ABS (C-P)			Ceramic-Polymer
CF-ABS (S2)			Mould Sealant 2
CF-ABS (E)			Epoxy-Based Sealant

Three unique tool substrate materials were used: Aluminum, glass-fibre epoxy (GF-Epoxy), and 20 wt% carbon-fibre reinforced acrylonitrile-butadiene-co styrene (CF-ABS). Aluminum and GF-Epoxy tools were traditional tooling options provided by an industrial partner to serve as benchmarks during testing, whereas CF-ABS tools were alternatively produced through a hybrid manufacturing process. It should be noted that, at the time of this publication, the subtractive component of the hybrid system was not fully operational, therefore the machining step was performed on a separate subtractive system (Struers Sectom-50). To prepare the hybrid manufactured tools, a hexagonal structure was printed and then machined and polished into the 25.4 mm x 25.4 mm tools, in which the surface perpendicular to the print direction was taken as the tool surface (Figure 2).

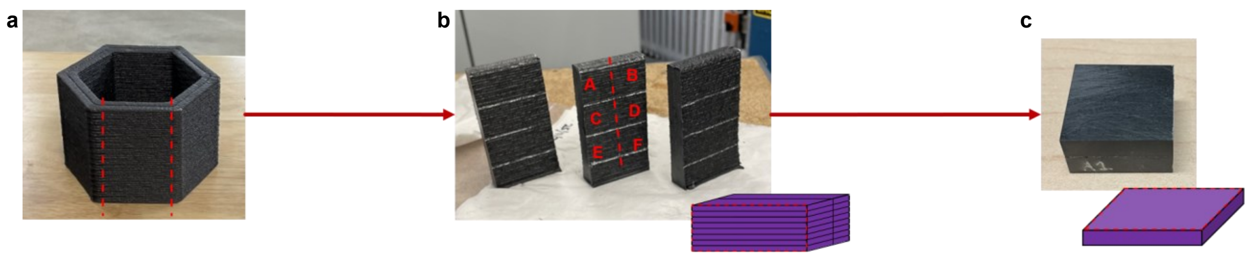

Figure 2. Manufacturing steps for tools produced through the hybrid manufacturing process. (a) A 2-bead thick hexagon is first printed in which the six sides are then cut to form (b) plates and subsequently (c) the 25.4 mm x 25.4 mm tools.

Following fabrication of the base tool substrates, 4 different coatings were applied to the specimens denoted as Sealant 1 (S1), Sealant 2 (S2), Ceramic-Polymer (C-P), and Epoxy-Based (E), while an additional set of hybrid manufactured tool substrates were left uncoated (U). Sealant 1 and Sealant 2 were both aerospace-grade mould sealants designed to fill in tool micro-porosity, resulting in an even surface to apply mould release. The Ceramic-Polymer coating was an epoxy-based coating containing ceramic nanoparticles that was advertised to offer superior mechanical and chemical wear resistance, used in applications ranging from consumer to aerospace. The final Epoxy-Based coating was an epoxy-based coating advertised to fill surface micro-porosity and provide a high gloss finish for additively manufactured parts.

2.2 Tensiometry

Advancing-receding contact angle (ARCA) optical tensiometry was employed to characterize the chemical resistance of the tools, correlating results to the tool's ability to resist bonding with composite parts during processing. Chemical resistance was specifically measured through dynamic contact angle hysteresis, in which a lower hysteresis value can then be attributed to the greater ability of the tool's surface to be nonstick [6]. The ARCA setup consisted of a 100 uL syringe (McMasterCarr) fitted with a 32 gauge needle (Nordson), with flow controlled by a syringe pump run using a custom Arduino script (Figure 3a). Reverse osmosis (RO) water was used as the droplet fluid, in which for each test a 2 uL droplet was first formed on the surface of each tool prior to the ARCA test (Figure 3bi). During each ARCA run, an additional 5 uL of RO water was injected during the advancing phase, followed by all water being drawn back into the syringe during the receding phase (Figure 3bii,iii). A high-speed camera (Infinity3-1UM) paired with standard video capture software (Lumenara Infinity Capture) was used for video acquisition of the advancing and receding droplet, the resulting data then processed (Photron FastCam Viewer 4) and analyzed (Dataphysics SCA 20) using tangent leaning fitting method to determine the advancing contact angle (ACA), receding contact angle (RCA), and hysteresis (i.e. difference between ACA and RCA) for each tool. A total of 2 samples were tested per tool, in which 3 ARCA measurements were performed on each.

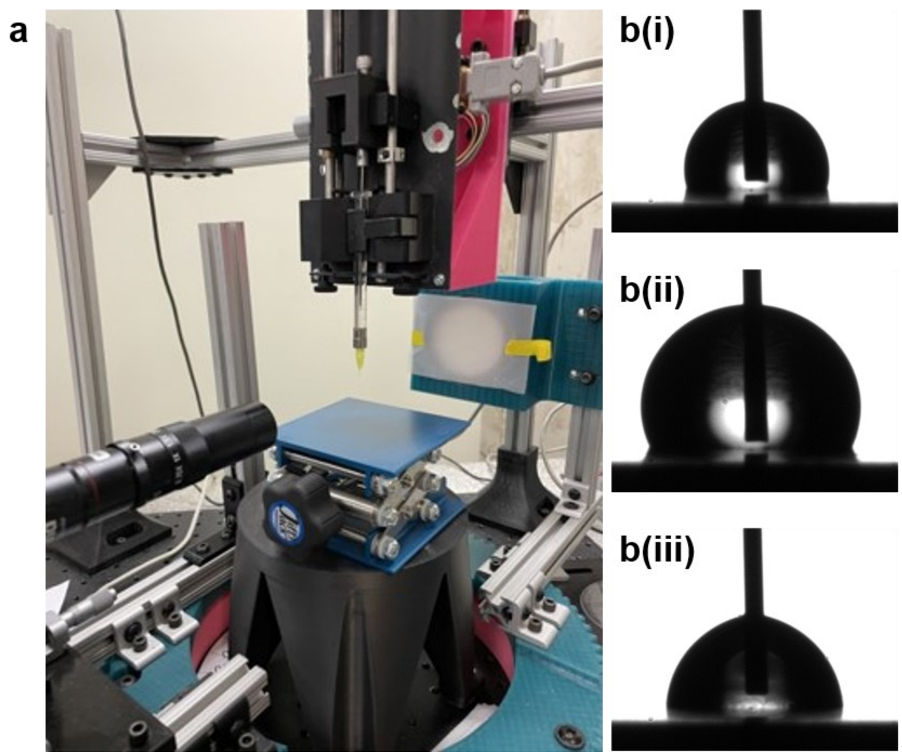

Figure 3. (a) Custom optical tensiometry setup. (bi-iii) The ARCA procedure beginning with (i) the initial droplet, (ii) the advancing droplet, and (iii) the receding droplet.

2.3 Vacuum Integrity

To assess the vacuum integrity of the fabricated tools a 5-minute "drop test" was performed on a custom vacuum fixture (Figure 4a). This fixture consisted of a small circular chamber of approximately 50.8 mm in diameter connected to a vacuum source controlled by an open close valve, a vacuum pressure gauge, and one other opening with a 19.05 mm x 19.05 mm to place the tool of interest. To use the fixture, at this opening, the tool of interest was secured using vacuum tape (General Sealants) as seen in Figure 4b, sealing off the cylindrical chamber when the vacuum source was closed. Vacuum was then drawn and the tool was further pressed into the vacuum tape to ensure a good seal. After maximum potential vacuum pressure was reached for a given tool (determined after no appreciable pressure change was observed for 2 minutes prior), the vacuum source was closed and the pressure was monitored over the 5-minute interval to obtain a "vacuum drop" value, calculated by taking the vacuum pressure at the start and end of the interval. A low vacuum drop was taken to be indicative that the given tool is impermeable to air, demonstrating good vacuum integrity (the converse being true for a tool with poor vacuum integrity). A total of 3 specimens were tested per tool. Prior to analysis of any tools, the fixture was first verified to have no other sources of vacuum pressure leak using nylon vacuum bag (Airtech).

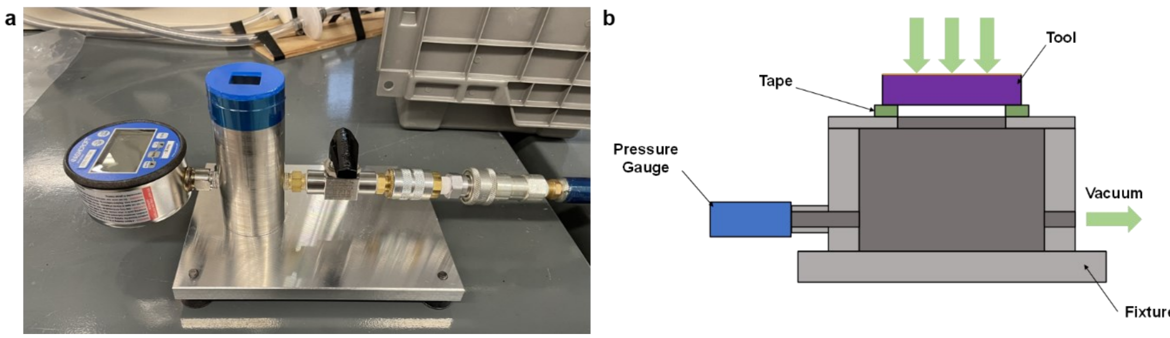

Figure 4. (a) Custom vacuum integrity setup and (b) its basic function. When vacuum is drawn in the chamber, the taped-down tool acts as the final wall of the chamber, any subsequent vacuum losses being attributed to permeability through the thickness of the tool.

2.4 Hardness/Micro-Indentation

Hardness values obtained through Vickers micro-indentation were correlated to the tool's ability to resist mechanical wear, with a specific focus on indentation caused by the fiber-reinforcement in composite parts during processing (Figure 5). A greater hardness would suggest greater resistance of the tool's surface to indentation. For each specimen, indentations into the surface were performed with a force of 50 mN, in which the loading time, holding time, and unloading time were each 30 seconds. These values were chosen based on literature previously reporting Vickers indentation on composite materials [7]. One specimen was tested per tool, in which twelve indentations were performed on each specimen in a 3 x 4 grid with indentation points separated by 100 microns in both the X and Y directions. Following each indentation, the geometry of each indentation was then analyzed to determine the hardness values.

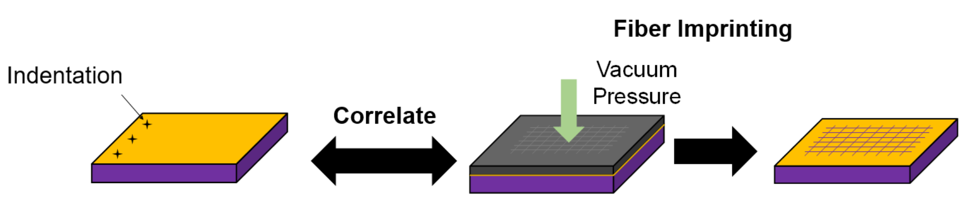

Figure 5. Correlation of tool hardness to mechanical resistance. During a composite process involving vacuum pressure, the vacuum pressure exerts a force that pushes the composite part into the tool. If the tool is not of sufficient hardness, this can lead to the imprinting of the fiber-reinforcement into the tool surface, leading to excessive mechanical wear.

3 RESULTS AND DISCUSSION

Results from the pre-screening tests show that though a tool could excel in one of the aforementioned categories (chemical resistance, vacuum integrity, mechanical resistance), it did not necessarily imply it's equal performance across all (Figure 6). Many of the tools, both traditional and hybrid, appeared to vary significantly in performance across the tensiometry, vacuum integrity, and hardness/micro-indentation tests, highlighting the importance of a small-scale test suite that characterizes tool durability on multiple fronts. The following subsections discuss findings relevant to each specific test before finally providing a structured framework in which to obtain a holistic interpretation of the results.

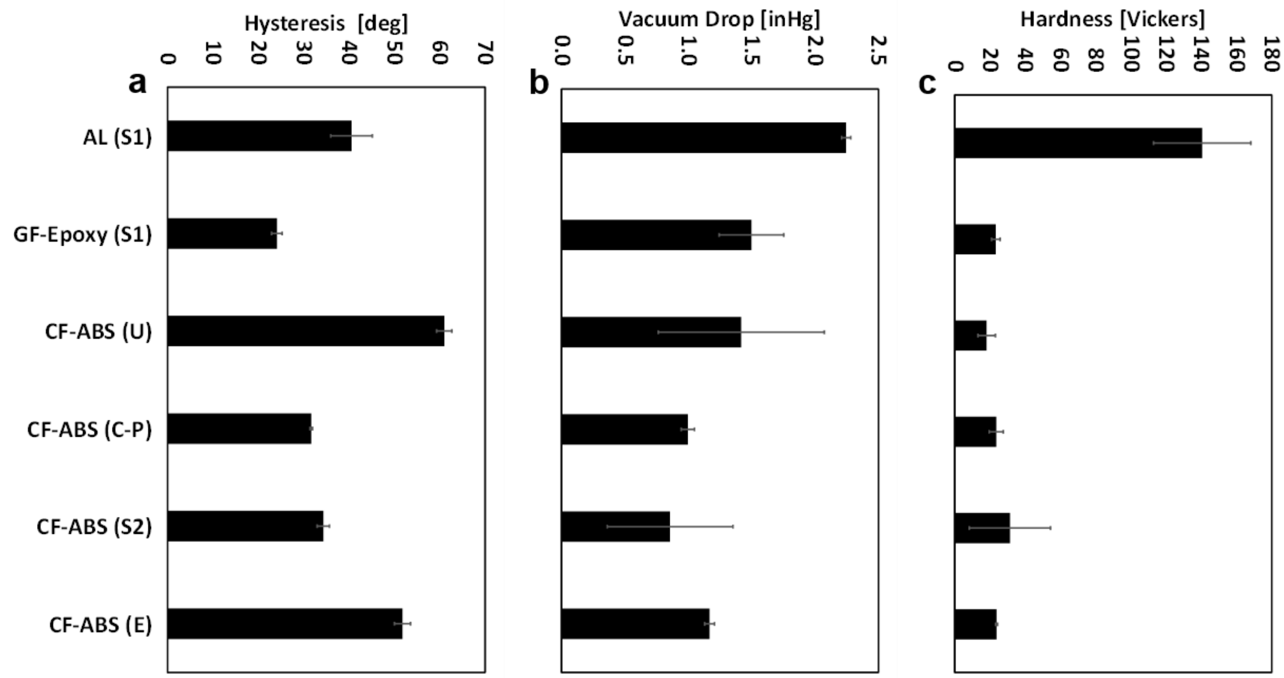

Figure 6. Pre-Screening Test Results. (a) Hysteresis, (b) Vacuum Integrity, (c) Hardness/Micro-Indentation.

3.1 Tensiometry

As seen in by the tensiometry results (Figure 6a), there was a spread of hysteresis values for tools suggesting varying degrees of chemical resistance. GF-Epoxy (S1) tools had the lowest hysteresis suggesting good nonstick properties, whereas CF-ABS (U) had the highest hysteresis and potentially the poorest nonstick properties. Interestingly, AL (S1) and GF-Epoxy (S1) tools had a large difference in hysteresis despite having the same coating. This difference in performance can potentially be explained by physical heterogeneity of the applied coating (i.e. an uneven/defective coating) due to surface roughness imparted by the underlying substrate [8] and/or repeatability of coating application. The resulting coating defects could ultimately lead to higher hysteresis values, and therefore lower chemical resistance.

For hybrid tools, CF-ABS (C-P) and CF-ABS (S2) had low hysteresis values relative to CF-ABS (U) and CF-ABS (E). Performance of the uncoated tool was predictable as it was not expected that the uncoated surface would possess any nonstick properties other than the effect of inherent surface roughness of the tool substrate [8]. Poor performance of CF-ABS (E) could potentially be explained by the previous findings between AL (S1) and GF-Epoxy (S1), specifically regarding an uneven/defective coating as it was seen following the application of the coating that bubbles formed on the surface, which could increase the hysteresis of the tool.

3.2 Vacuum Integrity

Vacuum integrity results across all tools show that CF-ABS (S2) had the lowest vacuum pressure drop, whereas AL (S1) had the highest (Figure 6b). Again, AL (S1) and GF-Epoxy (S1) tools had a large difference in hysteresis despite having the same coating, with AL (S1) tools experiencing almost complete vacuum drop for all tested tools. This is surprising as the AL (S1) tool is currently an industry standard. Variation between the two tools could instead potentially be explained by the same conclusions drawn for their performance in tensiometry. If the coating uniformity is compromised by poor coating application and/or influenced by underlying tool substrate roughness, this could lead to the ingress of air through the tool (if permeable) or between the tool and sealant tape due to high surface roughness that could create channels not sealed by the sealant tape. Regarding the latter, it is additionally probable that the adhesion between sealant tape and the tool surface was inherently poor as the bonding surface that the sealant tape was applied to was also treated with the S1 coating, which may also possess inherent nonstick properties. This could be relevant to all coated tools, and as such suggests that minor modification to the tools surface should be performed to keep the outer edges of the surface nonstick, promoting adhesion with the sealant tape.

Large standard deviation of CF-ABS (U) and CF-ABS (S2) can be attributed to incomplete removal of the layer lines of the additively manufactured structure during tool fabrication (Figure 7). When machining the 3D printed structure, if the surface is not milled sufficiently deep to reach the completely fused section of the layers there will be high surface roughness. This high surface roughness in turn could lead to easy access points for air ingress between the tool surface and sealant tape at the edges of the tool.

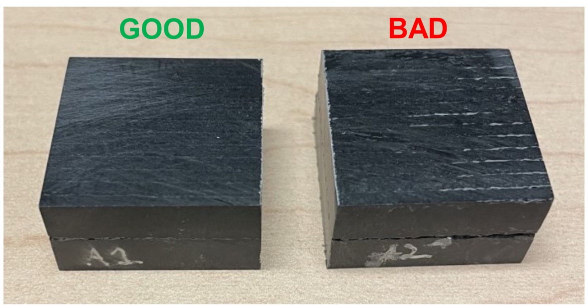

Figure 7. Effect of incomplete removal of layer lines on tool surface roughness.

3.3 Hardness/Micro-Indentation

Hardness/micro-indentation results show that AL (S1) tools exhibited the highest hardness, whereas CF-ABS (U) tools were the lowest (Figure 6c). The high hardness of the AL (S1) tool was expected, as it is the only tool material that was metal [9]. However, excluding the AL (S1) tool, the hardness values were relatively similar across all remaining tool types, the hybrid tools performing comparably to the traditional GF-Epoxy tool. It was not expected that S1 or S2 coatings provided much (if any) additional hardness to the tool substrates, as their primary function was to seal micro-porosity of the tool surface. The CF-ABS (S2) tool had the highest hardness of the hybrid manufactured tools, however the results had high standard deviation. High standard deviation of CF-ABS (S2) hardness values are thought to be a result of the location of indentation points for the given indenter type. When performing an indent on the hybrid manufactured tools, it is possible to indent on pure matrix, pure fibre, or a combination of both components (Figure 8). In the first two cases, the hardness would vary significantly due to the intrinsic hardness values of each material (i.e. matrix vs. fibre), ultimately leading to significant deviation for the final reported mean. This could potentially be mitigated in future work by utilizing an indenter type of sufficient size to ensure that each indentation point captures a similar distribution of fibres and matrix [10].

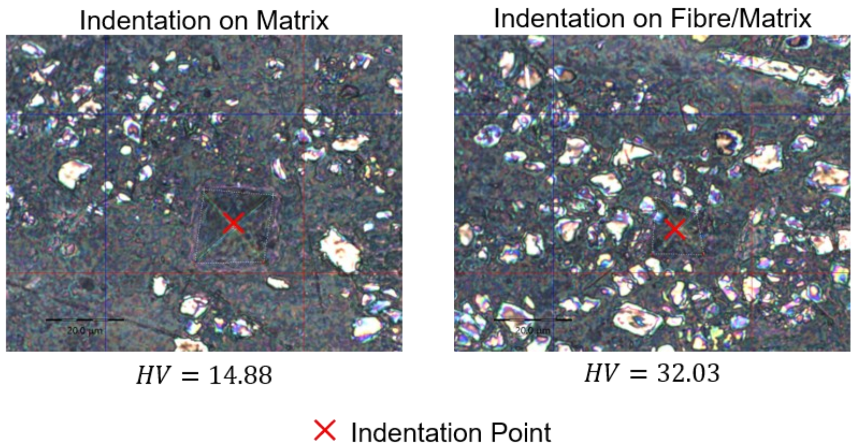

Figure 8. Variation of hardness due to indent location. Scale bar = 200 μm.

3.4 Analysis of Pre-Screening Tests

Upon collection of all the pre-screening test results, the analysis to determine the most optimal tool for the given application is accomplished in two distinct steps. In the first step, for each of the three pre-screening tests the results of each tool are ranked on an integer numeric scale ranging from 1 to the maximum number of tools ("n"), where 1 is the worst performing for the given test and "n" is the best performing for the given test. Following this ranking, the next step is to assign the relative weight of each of the three given pre-screening tests as a decimal number ranging from 0.0 (not important) to 1.0 (very important). The exact weight will depend on the specific application of the tool. The final step is to then calculate a performance index for each tool according to Equation 1:

$$Performance = \Sigma(Test\ Rank)_i(Test\ Weight)_i \quad , \quad i = \#\ of\ test\ methods \tag{1}$$

For each tool a single performance index is calculated by taking the summation of the rank obtained for each test by the associated test weight. The calculated performance indices can then be ranked in order of magnitude, with the highest value performance index representing the best tool for the given application (based on the weights given for each of the three pre-screening tests). Should the application change, the waiting can be reassigned for each test and the performance in the seas re-calculated for each tool and re-ranked to determine the new best tool.

The analysis of the pre-screening tests is presented in Table 2. Looking at the rank columns, it is apparent that the top-performing tool varied between each test. However, it did appear that some tools such as CF-ABS (C-P) and carbon CF-ABS (S2) did consistently rank higher than others. Using an equal weight for all tests (i.e. an application where all three properties characterized but each test are equally important), the performance index was calculated for each tool. From these performance indices, it can be seen that CF-ABS tools were ranked in the top two positions followed by a three-way tie by AL (S1), GF-Epoxy (S1), and CF-ABS (E) for third place.

Table 2. Analysis of the pre-screening test results.

Specimen ID	Tensiometry Rank	Vacuum Rank	Hardness Rank	Tensiometry Weight	Vacuum Weight	Hardness Weight	Performance
AL (S1)	3	1	6	1.0	1.0	1.0	10
GF-Epoxy (S1)	6	2	2				10
CF-ABS (U)	1	3	1				5
CF-ABS (C-P)	5	5	3				13
CF-ABS (S2)	4	6	5				15
CF-ABS (E)	2	4	4				10

A closer look at the performance indices shows that for some tools, despite having a high ranking, they did not perform significantly well in all tests. AL (S1) did not perform well in tensiometry or vacuum integrity, however it performed the best in hardness testing which significantly boosted its performance index. Similarly, GF-Epoxy (S1) did not perform well in vacuum integrity or hardness testing, but as the top-performing tool in tensiometry testing it likewise had an inflated performance index.

CF-ABS (S2) and CF-ABS (C-P) were the only tool that consistently ranked high for all three tests. These inflated performance indices are due to the fact that, for the given decision criteria, if a tool performs exceptionally well in at least one of the tests, it will have a high performance index even if it performs poorly in the others. As such, and improved decision criteria is needed to better assess tool results that considers the consistency in which the tool performs across all tests.

4 CONCLUSIONS & FUTURE WORK

Though the initial results of this work give important information regarding tool-coating performance at the small-scale, a few aspects of each test method need to be further improved to validate their use in predicting large-scale performance. Tensiometry results showed that contact angle hysteresis can potentially capture the tool’s ability to exhibit chemical resistance, however it is important to ensure sufficient surface/coating homogeneity to maximize this nonstick performance. Vacuum integrity tests offer a relatively simple method to characterize tool ability to maintain vacuum, however modification of the tool surface is needed to ensure that any vacuum pressure drop is exclusively due to tool permeability. Micro-indentation/hardness tests proved a quick and straightforward method to characterize tool mechanical resistance to indentation, however subsequent work requires an indenter of sufficient size to capture a more homogeneous picture of tool hardness. With these tests complete, it would additionally be important to perform a composite process using the tools to provide verification of their correlation to large-scale. Furthermore, future work in this area can draw from various other characterization techniques in the plethora of pre-existing characterization tools that exist, using them to address and quantitatively predict other fundamental properties of large-scale tooling at the small-scale.

5 ACKNOWLEDGEMENTS

The authors gratefully acknowledge the financial support provided by our partners at the Natural Sciences and Engineering Research Council of Canada (NSERC) and PRIMA Québec. The authors would also like to thank the support of the industrial partner for the assistance in preparing both traditional and hybrid tools, the McGill Biomimetic Surface Engineering Laboratory for their instruction on tensiometry testing, and the McGill Surface Engineering and Coating Tribology Laboratory for their assistance in performing hardness/micro-indentation testing.

6 REFERENCES

[1] CompositesWorld, "Materials & Processes: Tooling for composites," CompositesWorld, 23 03 2016. [Online].

[2] Pacific Aerospace Corp, "What Is Composite Layup Tool, and what are their benefits for Aerospace?," Pacific Aerospace Corp, 31 12 2021. [Online].

[3] N. Northrup, Durability of Hybrid Large Area Additive Tooling for Infusion of Composites, MSc, Brigham Young University, 2019.

[4] B. Post, B. Richardson, P. Lloyd, L. Love, S. Nolet and J. Hannan, "Additive Manufacturing of Wind Turbine Molds," Oak Ridge National Laboratory, Oak Ridge, 2017.

[5] T. Z. Sudbury, R. Springfield, V. Kunc and C. Duty, "An assessment of additive manufactured molds for hand-laid fiber reinforced composites," International Journal of Advanced Manufacturing Technology, vol. 90, no. 5-8, pp. 1659-1664, 2017.

[6] Y. Xiu, L. Zhu, D. W. Hess and C. P. Wong, "Relationship between Work of Adhesion and Contact Angle Hysteresis on Superhydrophobic Surfaces," Journal of Physical Chemistry C, pp. 11403-11407, 2008.

[7] F. Silva, R. Martinho, R. Alexandre and A. Baptista, "Increasing the wear resistance of molds for injection of glass fiber reinforced plastics," Wear, vol. 271, no. 9-10, pp. 2494-2499, 2011.

[8] H. Nakae, R. Inui, Y. Hirata and H. Saito, "Effects of surface roughness on wettability," Acta Materialia, vol. 46, no. 7, pp. 2313-2318, 1998.

[9] K.-H. Z. Gahr, "Chapter 2 Microstructure and Mechanical Properties of Materials," in Microstructure and Wear of Materials, Amsterdam, Elsevier, 1987, pp. 8-47.

[10] J. Lopez, "Microhardness testing of plastics: Literature review," Polymer Testing, vol. 12, no. 5, pp. 437-458, 1993.

[11] A. Hassen, J. Lindahl, X. Chen, B. Post, L. Love and V. Kunc, "Additive manufacturing of composite tooling using high temperature thermoplastic materials," in International SAMPE Technical Conference, Long Beach, 2016.